AVA sensitivity analysis and inversion of 3D pre-stack seismic data to delineate a mixed carbonate-siliciclastic reservoir in the Barinas-Apure Basin, Venezuela

Arturo Contreras and Carlos Torres-Verdín, The University of Texas at Austin*

Summary

Pre-stack seismic and well log data have been integrated through AVA seismic inversion to delineate a mixed carbonate-siliciclastic reservoir corresponding to the "O-Member" of the Escandalosa Formation in the Barinas-Apure Basin, Venezuela.

A detailed AVA sensitivity analysis was conducted to assess the nature of AVA effects in the study area. Such study included cross-plot analysis, Biot-Gassmann fluid substitution, AVA reflectivity modeling, and numerical simulation of synthetic gathers.

Although the AVA analysis indicates that the shale/carbonate interface represented by the top of the Escandalosa O-Member does not generate a significant AVA response, Biot-Gassmann analysis does show significant sensitivity of the modulus attribute ρf to fluid substitution. Accordingly, pre-stack seismic inversion results, which are layer dependent, have provided quantitative information about the lateral continuity of the carbonate reservoir as well as about the spatial distribution of economically viable areas, thereby significantly reducing exploration and development risk.

Introduction

The Barinas-Apure Basin, located in southwestern Venezuela, is one of the most prolific hydrocarbon-producing basins in Venezuela. Hydrocarbon production originates from reservoirs consisting of Tertiary siliciclastic deposits and Cretaceous carbonates. This paper considers a small portion of the Barinas sub-basin, in its northern flank, known as the Bejucal area, where oil-producing carbonates pertain to the "O" member of the Upper Cretaceous Escandalosa Formation and are buried at depths between 11100 and 11200 ft.

The "O" member of the Escandalosa Formation is a 70 to 80 feet thick mixed carbonate-siliciclastic interval composed of limestone, dolostone, arenitic dolostone, and calcareous sandstone, intercalated with shales and calcareous shales. The depositional setting is interpreted as a shallow-marine carbonate platform environment with variable input of siliciclasts. Significant surfaces have been interpreted as sequence boundaries that separate the basal "O" Member from the underlying "P" Member, and the upper "O" Member from the overlying La Morita Member of the Navay Formation (Figure 1b).

Due to depositional and diagenetic complexity, there is a wide range of pore types, including intercrystalline porosity, non-connected vuggy porosity, and fractures. Total porosity values are generally lower than 10%.

In an effort to substantially improve development in the study area and to evaluate the feasibility of new well locations we resorted to amplitude information of 3D pre-stack seismic data to quantify the vertical and lateral extent of the carbonate reservoir. We first conducted an AVO sensitivity analysis based on well-log data, and subsequently applied pre-stack seismic inversion to generate spatial distributions of fluid/solid sensitive modulus attributes.

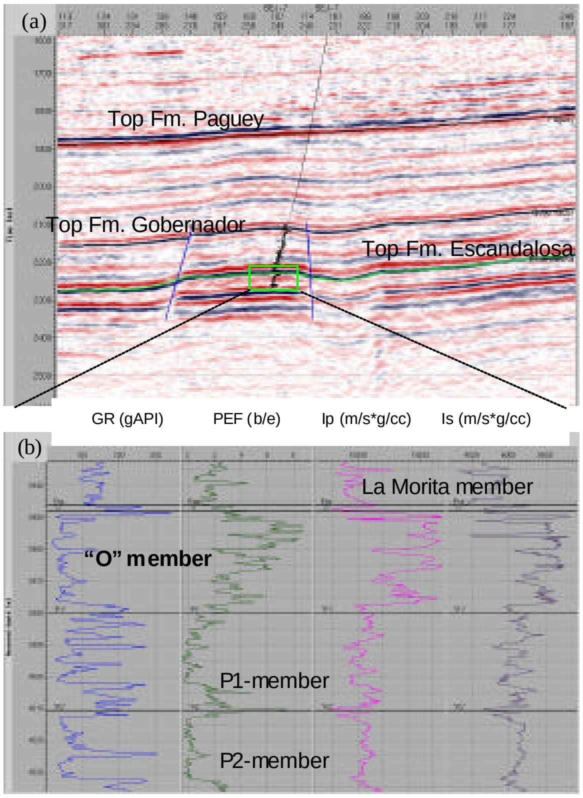

Figure 1: (a) Seismic cross-section in time with horizons interpreted to mark the tops of the main geologic formations (Paguey, Gobernador, and Escandalosa). (b) Example of wireline logs acquired in the same control well shown in Panel (a) and describing the characteristic high P- and S- impedance values across the "O" member.

AVA sensitivity analysis and inversion of 3D pre-stack seismic data to delineate a mixed carbonate-siliciclastic reservoir in the Barinas-Apure Basin, Venezuela

AVA Sensitivity Analysis

Wellbore data were analyzed to assess the AVA behavior of the Escandalosa Formation, and to determine the sensitivity of modulus attributes to changes in lithology and fluid content. Such sensitivity study consisted of (1) cross-plot analysis, (2) Biot-Gassmann fluid substitution, (3) AVA reflectivity modeling, and (4) numerical simulation of synthetic gathers.

Cross-plot analysis

P- and S-impedance (Ip and Is, respectively) being the product of the density times P- and S-velocity, respectively, were computed from dipolar sonic and density logs. Subsequently, the modulus attributes LambdaRho ($\lambda\rho$) and MuRho ($\mu\rho$) were computed and cross-plotted using $\lambda\rho=Ip^2-2Is^2$ and $\mu\rho=Is^2$. The effectiveness of this cross-plotting technique is based on the fact that $\lambda\rho$ is primarily sensitive to lithology, porosity, and fluid content, whereas $\mu\rho$ is primarily sensitive to lithology. Figure 2 shows a LambdaRho vs. MuRho cross-plot constructed with well-log data acquired in both O- and P-members of the Escandalosa Formation.

As indicated in Figure 2, carbonates and siliciclasts can be clearly differentiated on the basis of their modulus attributes $\lambda\rho$ and $\mu\rho$. Sands of the underlying Escandalosa "P-Member" are shown in blue, indicating low Photoelectric Factor (PEF), and corresponding to relatively low values of both $\lambda\rho$ and $\mu\rho$. Shales from both O- and P-Member are shown in green and exhibit intermediate values of PEF; their elastic behavior is characterized by relatively low values of both $\lambda\rho$ and $\mu\rho$. Limestones of the "O-member" are shown in yellow corresponding to high PEF values, and exhibit the largest values of $\lambda\rho$ and $\mu\rho$. Finally, dolomites having similar PEF values to those of shales are shown in green-red; they are represented by high values of $\lambda\rho$ and $\mu\rho$ but lower than those of limestones.

Although lithology discrimination can be performed on the basis of cross-plots similar to that shown in Figure 2, hydrocarbons (25 API oil) are known to be produced from dolomitized intervals, which clearly exhibit relatively low values of $\lambda\rho$.

Biot-Gassmann Fluid Substitution

Common wisdom dictates that, in general, pore-filling fluids have little or no effect on the effective elastic properties of carbonate rocks because of their relatively large elastic moduli. However, recent applications of AVO in carbonate reservoirs have shown that pore-filling fluids can have an appreciable effect on effective elastic properties (Li et al., 2003). To quantify the influence of saturating fluids on the acoustic properties of the "O-Member" reservoir rocks, fluid substitution analysis was performed based on the Biot-Gassmann equation for dolomitized intervals assuming a constant porosity of 10%.

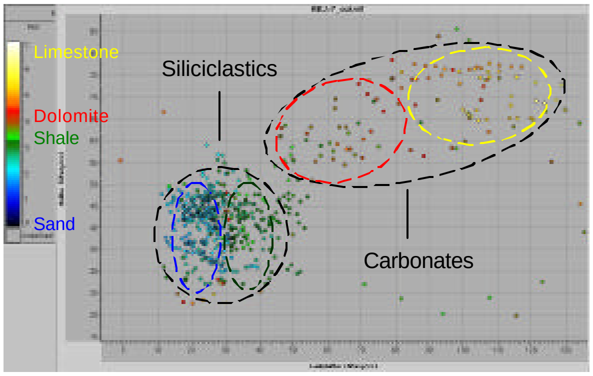

Figure 2: Cross-plot of LambdaRho ($\lambda\rho$) and MuRho ($\mu\rho$) crossplot using the logs in Figure 2(b). Siliciclastics and carbonates can be clearly discriminated.

Subsequently, a more generalized approach to fluid substitution was performed to compute the fluid factor attribute RhoFluid (ρf) introduced by Russell et al. (2003). The latter attribute is analogous to $\lambda\rho$ except that it enforces a relation equal to $=Ip^2-cIs^2$, where c is directly related to the Poisson's ratio of the dry rock frame or skeleton, i.e., $(\sigma_{dry}-1)/(\sigma_{dry}-0.5)$. In similar fashion, the solid factor attribute RhoSolid (ρs) is equivalent to $\mu\rho$. Recall that the lambda-mu-rho method uses a c value equal to 2, which implies a dry rock Poisson's ratio (σ_{dry}) of zero. For our fluid substitution analysis we used a value of σ_{dry} for limestone equal to 0.165, which corresponds to c=2.49.

Figure 3 shows the sensitivity of ρf and ρs to changes in water saturation and porosity. As expected, a significant reduction in the value of ρf ensues when replacing water with oil. Similarly, ρf decreases with an increase in porosity. This behavior indicates that, for the characterization of dolomite reservoirs, low values of ρf will be associated with highly-viable hydrocarbon-bearing rocks.

AVA Reflectivity Modeling

Well log data in combination with Zoeppritz equations were used to numerically model changes in PP reflectivity with incidence angle at the top of the "O-Member." The latter interface is a shale/carbonate contact. Results from this exercise are shown in Figure 4(a).

The simulated AVA reflectivity for Model No. 1 slightly decreases with angle for the angle-range contained in the seismic data. A significant increase in reflectivity occurs only for angles above the seismic range and toward the critical angle (~40°).

The main difference between the reflectivity behavior of O-member and Class 1 gas-sands is that the reflectivity of the Shale/O-member interface does not experience polarity reversals within the existing angle range. Consequently, neither "bright spots" nor "dim outs" associated with hydrocarbon replacement can be expected on stacked data at the shale/carbonate interface corresponding to the top of the "O" member".

Synthetic Gather Simulation

Synthetic gathers were simulated using well-log data from an oil-producing well. Such simulated gathers are the result of the convolution between a previously extracted wavelet and the well-log AVA reflectivity series, which in turn were computed from Vp, Vs, and density logs using the Knott-Zoeppritz equations. Results from the simulation of synthetic gathers are shown in Figure 4(b).

Consistent with the results of AVA reflectivity modeling, the synthetic gather simulation at the top of the O-member shows almost no amplitude-variations for the angle range contained in the seismic data. This flat behavior is corroborated by the measured angle gathers shown in Figure 4(c).

Pre-Stack Seismic Inversion

Four partial angle stacks were simultaneously inverted using an AVA constrained sparse spike inversion (CSSI) algorithm. AVA simultaneous inversion combines the advantages of AVA analysis with those of inversion. While standard AVA analysis renders information about rock interfaces, inversion yields information about rock layers. The inversion methodology consisted of partial angle stacking, low frequency modeling, wavelet estimation, AVA-CSSI simultaneous inversion, inversion quality control, and attribute extraction. The two main inversion products, P- and S-impedance, were used to generate volumes of the modulus attributes ρs and ρf using the weighting factor c=2.49 used in the fluid substitution exercise.

Maps of RMS modulus attributes ρs and ρf were subsequently generated from the stratigraphic interval of the O-member. Figure 5(a) is a 3D view of the structural map in time corresponding to the top of the O-member. Similarly, Figures 5(b) and 5(c) show final maps pf ρs and ρf overlaying the same time horizon displayed in Figure

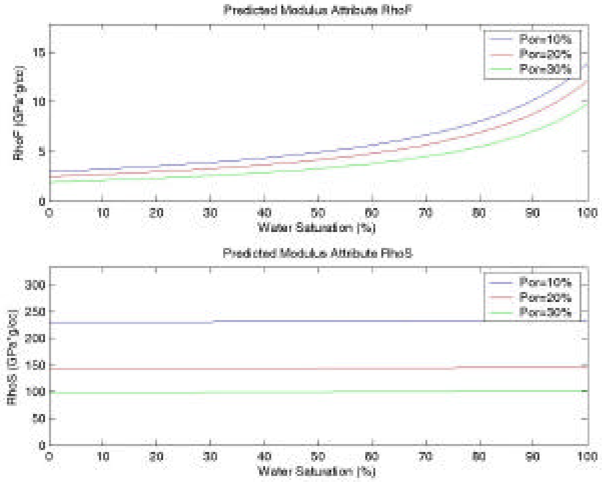

Figure 3: Modulus attributes RhoF (ρf) and RhoS (ρs) as functions of water saturation for different values of porosity (dolomite matrix). The modulus ρf decreases with hydrocarbon saturation, whereas ρs remains insensitive to fluid substitution. Both modulus attributes decrease with increasing porosity.

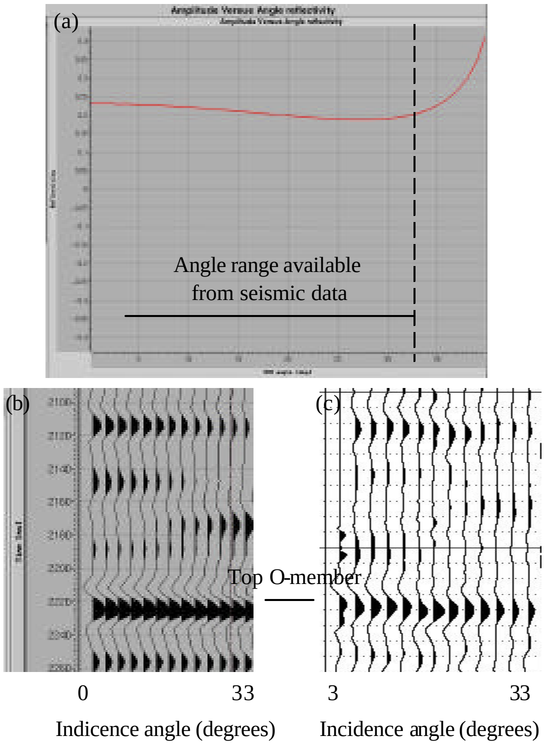

Figure 4: (a) Reflectivity modeling of the Shale/O-member interface; (b) synthetic angle gather; and (c) measured angle gather. No significant AVA effect is produced by the Shale/O-member interface.

5(a). The $\mu\rho$ attribute, which is primarily sensitive to the rock's solid framework, is extremely valuable for geological modeling: relatively high values of $\mu\rho$ are associated with carbonate rocks whereas relatively low values of $\mu\rho$ indicate an increase in the rock's clastic content.

The ρf attribute, which remains sensitive to the rock's fluid component, is extremely valuable for delineation of hydrocarbon-bearing rocks. As mentioned before, the Biot-Gassmann fluid substitution exercise indicates that hydrocarbon replacement on a water-saturated dolomite decreases the value of ρf. The maps shown in Figure 59(c) clearly confirm that the range of values spanned by ρf correlates with well production data. Accordingly, oil-producing wells (shown with green lines) are located over or on the boundaries of low ρf anomalies, whereas dry or very low producing wells (shown with blue lines) coincide with high ρf anomalies.

In addition to well production data, the accuracy and reliability of the inversion results was validated in three ways: (a) through a detailed sensitivity analysis of the inversion residuals, (b) with an exhaustive perturbation analysis of all of the inversion parameters, and (c) with inversion exercises performed on multiple combinations of angle ranges.

Conclusions

Standard AVA analysis indicates that the shale/carbonate interface represented by the top of the Escandalosa O-Member does not generate significant AVA anomalies. However, pre-stack seismic inversion results combined with well-log data do provide quantitative information about the spatial continuity of the reservoir and of its hydrocarbon-bearing rocks. This is attributed to the fact that AVA produces information about rock interfaces (shale/O-member) whereas inversion produces information about rock layers (O-member). In addition, Biott-Gassmann fluid substitution indicates that fluids do affect the acoustic response of dolomites, and the corresponding effect can be accurately quantified through fluid/solid-sensitive attributes such as ρf. By combining AVA sensitivity analysis techniques with pre-stack seismic inversion, geologic/production data, and awareness of inversion pitfalls, it is possible to substantially reduce the risk in exploration and development of the O-Member reservoir.

Acknowledgments

The authors would like to thank PDVSA for providing the data set used for the research study described in this paper. A note of special gratitude goes to Fugro-Jason for their unrestricted software support.

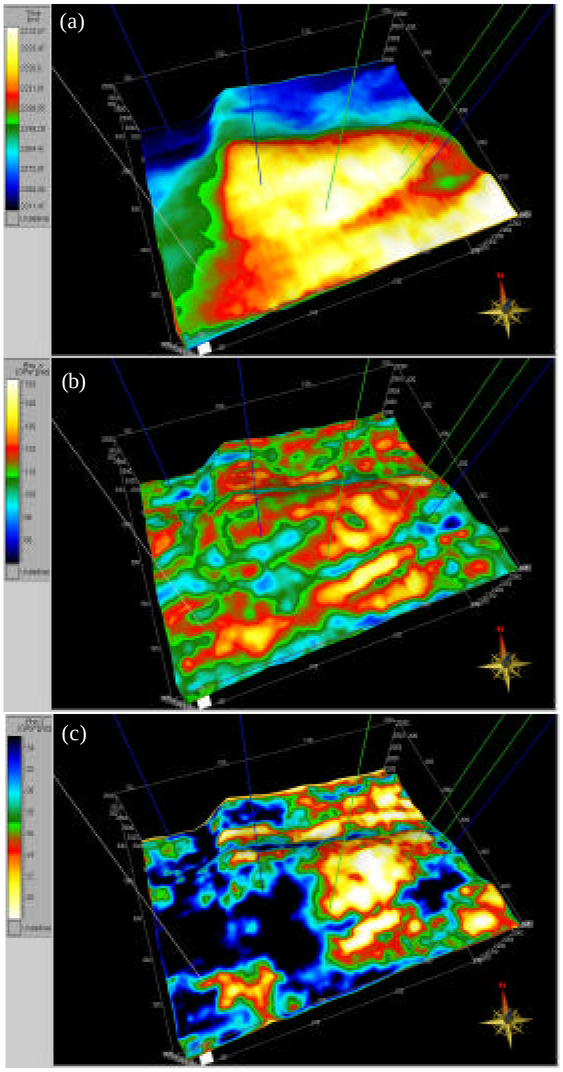

Figure 5: (a) Structural map in time for the top of the "O" member; (b) RMS map of ρs for the "O" member; (c) RMS map of ρf for the "O" member. Green lines represent hydrocarbon-producing wells; blue lines: dry wells; white line: not tested well. Most prospective areas are associated with low ρf anomalies. (Area $\cong$ 30 km^2).

References

Li, Y., Downton, J., and Goodway, B., 2003, Recent applications of AVO to carbonate reservoirs in the Western Canadian Sedimentary Basin, The Leading Edge, 670-674.

Russell, B., Hedlin B., Hilterman, F., and Lines, L., 2003, Fluid-property discrimination with AVO: A Biot-Gassmann perpective, Geophysics, Vol. 68, No. 1, 29-39.